Eur. Phys. J. B **3**, 407–411 (1998)

THE EUROPEAN PHYSICAL JOURNAL B

Magic numbers in vertically coupled quantum dots

W.-Y. Ruan[1,a] and H.-F. Cheung[2]

[1] Department of Applied Physics, South China University of Technology, Guangzhou 510641, P.R. China
[2] Department of Physics and Material Science, City University of Hong Kong Kowloon, Hong Kong

Received: 13 July 1997 / Accepted: 7 October 1997

Abstract. A coupled quantum dot system has been studied by numerical diagonalization of the Hamiltonian. Discontinuous ground-state transitions induced by an external magnetic field have been predicted. Series of magic numbers of angular momentum which minimize the ground-state electron-electron interaction energy have been discovered. Theoretical explanations derived from the first principles have been formulated.

PACS. 73.20.Dx Electron states in low-dimensional structures (superlattices, quantum well structures and multilayers) – 73.20.Mf Collective excitations (including plasmons and other charge-density excitations) – 73.40.Kp III-V semiconductor-to-semiconductor contacts, p-n junctions, and heterojunctions

In recent years, advances in nanofabrication technology have allowed the creation of artificial semiconductor structures containing only a small number of electrons, called quantum dots [1]. Recent experimental work has explored phenomena such as quantum dot charging [2], transport through quantum dots [3,4], and far-infrared absorption [5]. Specifically, the single-electron capacitance spectroscopy allows the direct measurement of energies of quantum levels of the dot as a function of magnetic field [2]. Related theoretical studies have led to interesting predictions of the existence of magic angular momentum for interacting electrons in the dots [6–11]. In fact they are the possible angular momenta only where the ground state can occur if a dot is placed in a magnetic field. Transitions from one magic value to another can be induced by changing the magnetic field. Recently these predictions have been confirmed unambiguously by experiments for dots with $N = 2, 3$ [12]. In this paper, we studied the coupled quantum dots by exact numerical diagonalization and predicted novel ground-state transitions. The model has been previously studied partly (polarized states) [13], by using the perturbative method and the unphysical inverse-square potential, β/r^2, for particle-particle interactions. In this work, we consider all the spin configurations and the particle-particle interaction used in the calculation is the unscreened Coulomb potential. The introduction of 2D harmonic oscillator transformation bracket allows us to evaluate the H matrix analytically. As we will show in the following that the appearance of magic numbers in coupled dots can be understood as the results of symmetry constraints.

[a] e-mail: phwyruan@scut.edu.cn

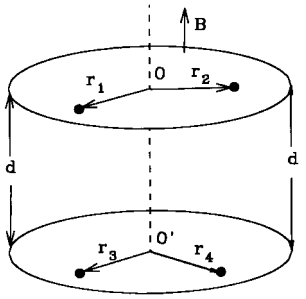

Fig. 1. Schematic configuration of two coupled quantum dots.

Consider a system of two adjacent, collinear quantum dots as schematically shown in Figure 1. We assume that each quantum dot contains only two electrons. Such a system is the simplest including both intradot and interdot interactions. The confinement potential, as is appropriate for the experiment, is taken to be parabolic, $\frac{1}{2}m^*\omega_0^2 r^2$ [7–12], where m^* is the effective electron mass, ω_0 is a strength parameter for the confinement potential. The external magnetic field is assumed to be along the $-z$ direction. The electron-electron interaction is taken to be the unscreened Coulomb potential. The electron tunnelings between two dots are assumed to be negligible. The Hamiltonian is given by

$$H = \sum_{i=1}^{4}\left[\frac{1}{2m^*}(\mathbf{p}_i + e\mathbf{A})^2 + \frac{1}{2}m^*\omega_0^2 r_i^2\right] + V_{intra} + V_{inter} + g^*\mu_B B S_z \quad (1)$$

where V_{intra} and V_{inter} are respectively the intradot and interdot electron-electron interactions,

$$V_{intra} = \frac{e^2}{4\pi\epsilon_0\epsilon_r}\left[\frac{1}{r_{12}} + \frac{1}{r_{34}}\right] \tag{2}$$

$$V_{inter} = \frac{e^2}{4\pi\epsilon_0\epsilon_r}\left[\frac{1}{\sqrt{r_{13}^2+d^2}} + \frac{1}{\sqrt{r_{14}^2+d^2}} + \frac{1}{\sqrt{r_{23}^2+d^2}} + \frac{1}{\sqrt{r_{24}^2+d^2}}\right]. \tag{3}$$

With symmetric gauge $\mathbf{A} = \mathbf{B}\times\mathbf{r}/2$, equation (1) can be rewritten into

$$H = \sum_{i=1}^{4}\left[\frac{p_i^2}{2m^*} + \frac{1}{2}m^*\omega_B^2 r_i^2\right] + V_{intra} + V_{inter} + \frac{\omega_c}{2}L_T + g^*\mu_B B S_z \tag{4}$$

where $\omega_B = \sqrt{\omega_0^2 + \omega_c^2/4}$, $\omega_c = eB/m^*$ is the cyclotron frequency, L_T is the total orbital angular momentum (including the center-of-mass' and the relative) in the z direction, g^* is the effective Lande factor, S_z is the z component of the total spin.

Significant simplification of equation (4) can be achieved by introducing a set of center-of-mass and canonical relative coordinates: $\mathbf{R}_{cm} = \sum_{i=1}^{4}\mathbf{r}_i/4, \xi_1 = (\mathbf{r}_1 - \mathbf{r}_2)/2, \xi_2 = (\mathbf{r}_3 - \mathbf{r}_4)/2, \xi_3 = (\mathbf{r}_3 + \mathbf{r}_4 - \mathbf{r}_1 - \mathbf{r}_2)/2$. Equation (4) can then be divided into two independent parts

$$H = H_{cm} + H_r \tag{5}$$

with

$$H_{cm} = \frac{P_{cm}^2}{2M} + \frac{1}{2}M\omega_B^2 R^2 + \frac{\omega_c}{2}L_{cm} \tag{6}$$

$$H_r = H_0 + V_{intra} + V_{inter} \tag{7}$$

$$H_0 = \sum_{\nu=1}^{3}[\frac{p_\nu^2}{2\mu_\nu} + \frac{1}{2}\mu_\nu\omega_B^2\xi_\nu^2] + \frac{\omega_c}{2}L + g^*\mu_B B S_z \tag{8}$$

where H_{cm} describes the center-of-mass motion, H_r describes the relative motion, $M = 4m^*$ is the total mass, $\mu_1 = \mu_2 = m^*/2, \mu_3 = m^*$, L_{cm} and L are the angular momentum operators associated with the center-of-mass and relative motions respectively. The eigensolutions of H_{cm} are obviously the ordinary 2D harmonic oscillator functions.

To obtain the eigenfunctions and eigenenergies associated with the relative motion, we diagonalized H_r in a model space spanned by the translationally invariant 2D harmonic product basis states $\{\Phi_{[k]} \equiv \phi_{n_1 l_1}(\xi_1)\phi_{n_2 l_2}(\xi_2)\phi_{n_3 l_3}(\xi_3)\}$, where $[k]$ denotes the whole set of quantum numbers $(n_1, l_1, n_2, l_2, n_3, l_3)$ in brevity. The angular quantum number $l_1 = odd$ if the spin of particle cluster (e_1, e_2) $S_{12} = 1$, and $l_1 = even$ if $S_{12} = 0$; similar restrictions apply for l_2 such that the full wavefunction is properly antisymmetrized. The matrix elements of H_r are then given by the following expressions,

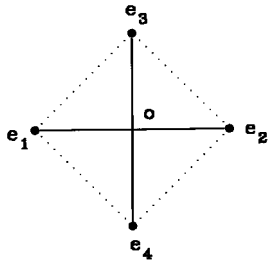

Fig. 2. Projection of the equilibrium configuration of the system on to an $x-y$ plane. The dotted lines constitute a square. Particle pairs (e_1, e_2) and (e_3, e_4) are on a different $x-y$ plane.

$$\langle\Phi_{[k]}|H_0|\Phi_{[k']}\rangle = \Big\{[2(n_1+n_2+n_3) + |l_1| + |l_2| + |l_3| + 3]\hbar\omega_B + \frac{\omega_c}{2}L + g^*\mu_B B S_z\Big\}\delta_{[k],[k']} \tag{9}$$

$$\langle\Phi_{[k]}|V_{intra}|\Phi_{[k']}\rangle = U^I_{n_1 l_1, n_1' l_1'}\delta_{l_1,l_1'}\delta_{n_2,l_2'}\delta_{l_2,l_2'}\delta_{n_3,n_3'}\delta_{l_3,l_3'} + U^I_{n_2 l_2, n_2' l_2}\delta_{n_1,n_1'}\delta_{l_1,l_1'}\delta_{l_2,l_2'}\delta_{n_3,n_3'}\delta_{l_3,l_3'} \tag{10}$$

$$\langle\Phi_{[k]}|V_{inter}|\Phi_{[k']}\rangle = 4\sum_{[k'']}\sum_{[k''']} A_{[k],[k'']}A_{[k'],[k''']} \times U^{II}_{n_1'' l_1'', n_1''' l_1'''}\delta_{l_1'',l_1'''} \times \delta_{n_2'',n_2'''}\delta_{l_2'',l_2'''}\delta_{n_3'',n_3'''}\delta_{l_3'',l_3'''} \tag{11}$$

with

$$U^I_{nl,n'l} = \int_0^\infty R_{nl}(\xi)\frac{e^2}{4\pi\epsilon_0\epsilon_r\xi}R_{n'l}(\xi)\xi d\xi \tag{12}$$

$$U^{II}_{nl,n'l} = \int_0^\infty R_{nl}(\xi)\frac{e^2}{4\pi\epsilon_0\epsilon_r\sqrt{\xi^2+d^2}}R_{n'l}(\xi)\xi d\xi \tag{13}$$

$$A_{[k],[k']} = \int \Phi_{[k]}(\xi_1,\xi_2,\xi_3)\Phi_{[k']}(\xi_1',\xi_2',\xi_3')d\xi_1 d\xi_2 d\xi_3 \tag{14}$$

where R_{nl} is the radial part of 2D harmonic oscillator function, $A_{[k],[k']}$ is the transformation bracket of 2D harmonic product states with two different sets of relative coordinates for four-body systems, which allows us to reduce the otherwise multi-integral into single-integral. Nonvanishing $A_{[k],[k']}$ occurs only when both the states $\Phi_{[k]}(\xi_1,\xi_2,\xi_3)$ and $\Phi_{[k']}(\xi_1',\xi_2',\xi_3')$ have the same eigenenergy and eigen angular momentum. Analytical expression for $A_{[k],[k']}$ has already been derived in reference [14]. The set of canonical coordinates $\{\xi_1',\xi_2',\xi_3'\}$ are defined by $\xi_1' = (\mathbf{r}_1 - \mathbf{r}_3)/2, \xi_2' = (\mathbf{r}_2 - \mathbf{r}_4)/2, \xi_3' = (\mathbf{r}_2 + \mathbf{r}_4 - \mathbf{r}_1 - \mathbf{r}_3)/2$. In our practical diagonalizations, basis states from six Landau levels were included.

Unlike a classical mechanical system, the behaviour of a quantum system is governed both by the dynamical properties (particle masses, details of the interactions) and by the exchange symmetry of the constituents. As we will show in the following, the later is more important a factor responsible for the phenomena we are focusing on.

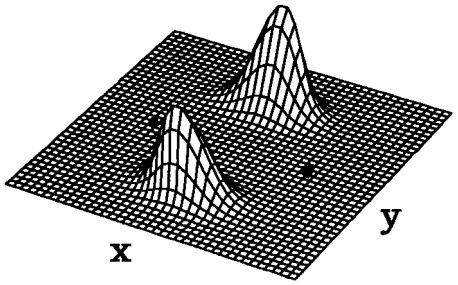

(a)

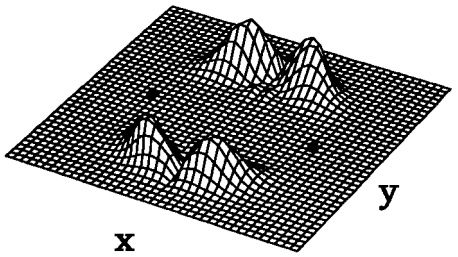

(b)

Fig. 3. Density distribution of the lowest state with (a) magic L; (b) non-magic L as a function of (x_1, y_2). The two black dots are positions of particles e_3 and e_4 with the optimized separation. We set $(x_2, y_2) = (-x_1, -y_1)$ such that the center-of-mass of the global system is fixed at the center.

Therefore, before going to the details of the numerical results, let us first investigate the constraints that antisymmetrization imposes on the geometrical configuration of a strongly correlated system. The equilibrium configuration of the present system is schematically shown in Figure 2. This is a square with the particles at the vertexes when their positions are vertically projected onto the same $x-y$ plane. Actually the particle pairs (e_1, e_2) and (e_3, e_4) are on a different $x-y$ plane (see Fig. 1). Hence we call this configuration a pseudo-square (PS) hereafter. In quantum mechanics, a system can not possess a rigid geometrical shape as its classical correspondent does, instead, we have a distribution of the probability density. However, in order to minimize the interaction energy, the distribution of the wavefunction of the ground state should be smoothly (without nodal lines) peaked at the PS. We notice that with the PS configuration a rotation of 180° is equivalent to the particle exchange $1 \leftrightarrow 2$, and $3 \leftrightarrow 4$. Let Ψ_L be the spatial part of the wavefunction with angular momentum L, $\Psi_L(PS)$ be the probability amplitude for the four particles to form a PS. Then this can be expressed as

$$R_{180^\circ}\Psi_L(PS) = P_{(12)(34)}\Psi_L(PS). \qquad (15)$$

When acting on the wavefunction, the operator R_{180° produces a factor of $(-1)^L$, while $P_{(12)(34)}$ produces a factor of $(-1)^{S_{12}+S_{34}}$ such that the full wavefunction (a product of the spatial part and the spin part) is antisymmetric.

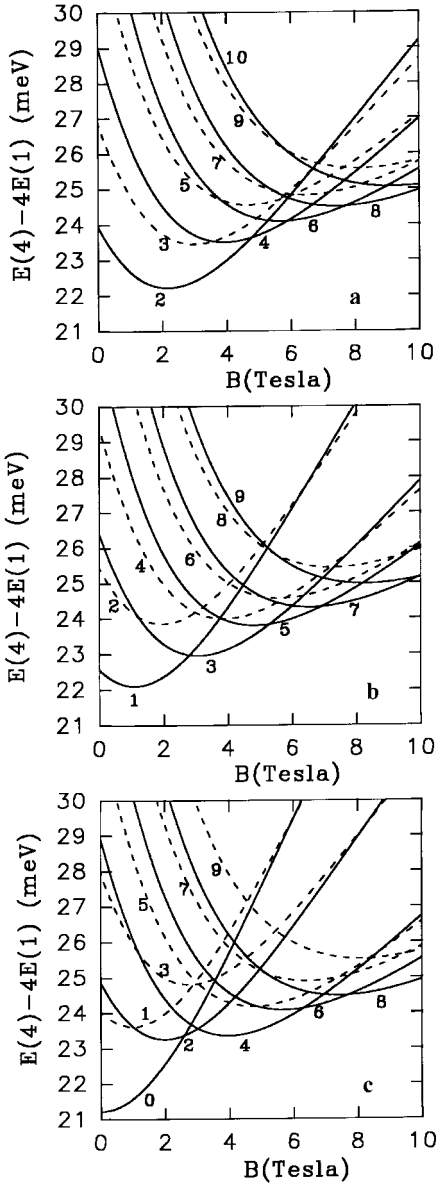

Fig. 4. The lowest state of a L as a function of the magnetic field, a). $S_{12} = S_{34} = 1$, b). $S_{12} \neq S_{34}$, c). $S_{12} = S_{34} = 0$. The solid lines are associated with magic L, the dashed lines are associated with non-magic L. The numbers in the figures label the angular momentum of the state. Parameters are taken appropriate for GaAs. $\hbar\omega_0 = 3.6$ meV, $d = 2l_0$ ($l_0 \equiv \sqrt{\hbar\omega_0/m^*}$).

Hence equation (15) can be rewritten into

$$\left[(-1)^L - (-1)^{S_{12}+S_{34}}\right]\Psi_L(PS) = 0. \qquad (16)$$

This implies that the most favourable PS configuration is completely prohibited (*i.e.*, $\Psi_L(PS) = 0$) by symmetries unless L takes the *magic* values fullfilling $(-1)^L = (-1)^{S_{12}+S_{34}}$, *i.e.*, $L = even$ if $S_{12} = S_{34}$, and $L = odd$ if $S_{12} \neq S_{34}$ ($S_{12}, S_{34} = 0, 1$). (More generally speaking, it is the pseudo-diamond (PD) that is prohibited, the PS is

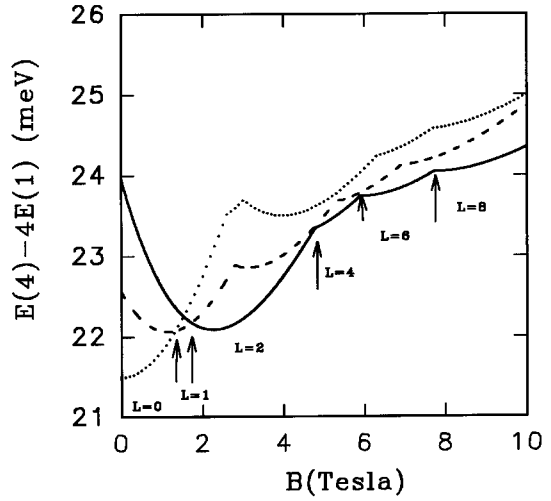

Fig. 5. The lowest energy of a spin configuration as a function of the magnetic field: $S_{12} = S_{34} = 1$, solid curve; $S_{12} \neq S_{34}$, dashed curve; $S_{12} = S_{34} = 0$, dotted curve.$S_z = S_{12} + S_{34}$ in all cases. Arrows point to the position where a ground-state angular momentum and/or spin transition occurs.

a special case of which.) With this in mind, we presented the numerical results as follows.

1. To see intuitively the effect of PS prohibition. We set the positions of particle e_3 and e_4 to $(x_3, y_3) = (a, 0)$ and $(x_4, y_4) = (-a, 0)$ respectively, where a is the optimized value of particle separation. We further set $(x_1, y_1) = (-x_2, -y_2)$. Then the density function $|\Psi_L|^2$ of the lowest states are plotted as a function of (x_1, y_1) in Figures 3. Figure 3a is a state with a magic L, Figure 3b is a state with non-magic L. In Figure 3a the density function concentrates to the positions $(0, \pm a)$, implying that the PS configuration is strongly pursued to successfully minimize the interaction energy, while in Figure 3b the y-axis is a nodal line of the wavefunction preventing the four particles from forming a PD configuration. Since the curvature of the wavefunction increases with the number of nodes, the appearance of this nodal line is energetically quite unfavorable. Consequently the state will be prevented from becoming the ground-state (see below).

2. In Figures 4 we presented the energy of the lowest state of an L as a function of the external magnetic field B separately for each spin configuration. The terms of E_{cm} and $g^*\mu_B B S_z$ are not included here. It is the competition between the single particle energy and the interaction energy that finally determines the total energy. The existence of the Zeeman term $\omega_c L/2$ (negative) enables states with larger L to be possibly even lower than those with smaller L . As a result, the lowest state for a given spin configuration occurs at larger L as the magnetic field increases. However, the transition is strictly restricted to between two magic numbers of L. States with non-magic L lie much higher and are excluded from becoming the lowest of the spin configuration due to the existence of PS prohibition and the failure to minimize the interaction energy.

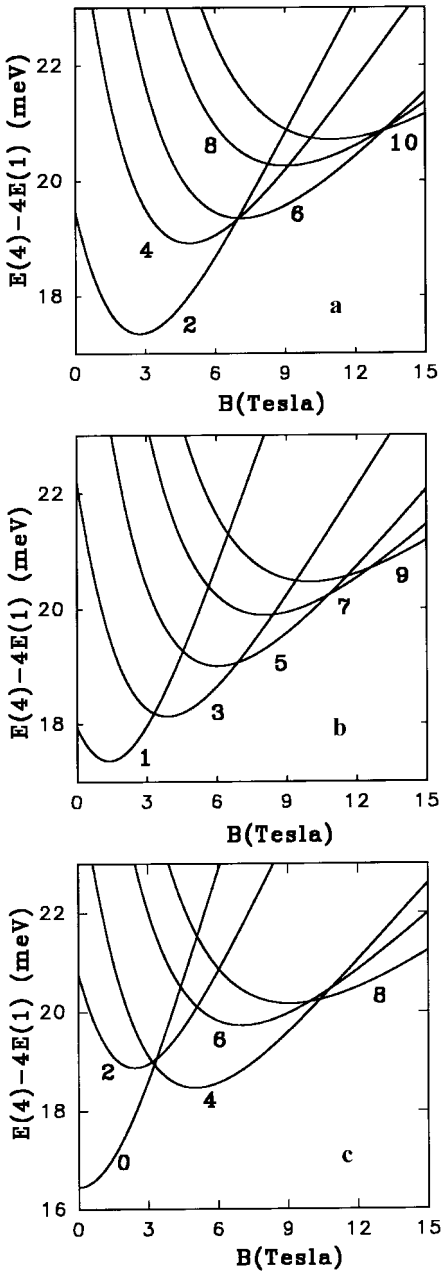

Fig. 6. The same as Figures 4 except for $d = \infty$.

In Figure 5, the lowest energy of a spin configuration was presented as a function of the external magnetic field. Unlike Figure 4, the spin-dependent term $g^*\mu_B B S_z$ has been included here (we always set $S_z = S_{12} + S_{34}$), which advantages the spin-polarized states. Consequently, ground-state spin transitions $S = 0 \to 1 \to 2$ occur in the range between $B = 1$ and 2 (Tesla). Over that region, the magnetic field is strong enough to keep the system fully polarized and the ground state runs only on the magic L's associated with the spin configuration $S_{12} = S_{34} = 1$.

3. It is interesting to compare the above results with those when $d \to \infty$ and the two dots become independent (see Figs. 6). In this case, the angular momentum of each

single dot (L_{12} or L_{34}) is a good quantum number. The two-electron single dot system has been studied in great detail by Merkt *et al.* [15]. As is required by the Pauli principle, $L_{12} = 2k+1$ (k=0, 1, 2...) if $S_{12} = 1$ and $L_{12} = 2k$ if $S_{12} = 0$. In Figure 6a and c where $S_{12} = S_{34}$, the possible lowest states occur only at those satisfying the Pauli principle and $L_{12} = L_{34}$, *i.e.*, $L = 2(2k + 1)$ for $S_{12} = S_{34} = 1$ and $L = 4k$ for $S_{12} = S_{34} = 0$. For $S_{12} = S_{34} = 1$, the sequence $L = 4k$, which can become the lowest state in coupled dots, fails to become the lowest state in uncoupled dots. For $S_{12} = S_{34} = 0$, it is the sequence $L = 2(2k + 1)$ that fails to become the lowest state in uncoupled dots. For $S_{12} \neq S_{34}$, it is not allowed to have $L_{12} = L_{34}$ and the possible lowest states are of the same as those of coupled dots.

4. Of the aboved calculations, two extensions have been done by assuming different sizes of the two dots and by taking nonparabolic confinements. When the two dots are different in size, the most favourable configuration of the system is a PD, for which equation (15) continues to hold. For nonparabolic dots the center-of-mass mode of motion is coupled with the relative motion. We found that the qualitative feature is of the same as discussed above since the symmetry constraints are of the same.

To summarize, we have numerically diagonalized the Hamiltonian of two coupled quantum dots and analyzed the low-lying states systematically. Similar to a single dot, the ground state of a two-coupled-dot system varies discontinuously in a magnetic field, showing a selection rule for the total angular momentum L. The interdot correlation leads to some extra sequences of possible ground states which do not exist in uncoupled dots. There is a reminiscence of the $\nu = 1/2$ fractional quantum Hall effect in double layers of electrons in strong magnetic field, induced by interlayer correlations. For the appearance of magic numbers in coupled quantum dots, we have argued that this be due to the particle-particle interaction and symmetry constraints solely and have very little to do with the dynamical properties. With our theory, all the magic L can be derived algebraically and simply. Since now several experimental methods have been developed to probe the ground state energy of quantum dots, what we have found here may be put to test in experiments in the near future.

This work is supported by the Research Committee, City University of Hong Kong, under grant No. 7000415, Guangdong Provincial Natural Science Foundation and Guangzhou Civic Natural Science Foundation.

References

1. M.A. Kastner, Phys. Today, **46,** 24 (1993).
2. R.C. Ashoori, *et al.*, Phys. Rev. Lett. **71,** 613 (1993).
3. P.L. McEuen, *et al.*, Phys. Rev. Lett. **66,** 1296 (1991).
4. J. Weis, *et al.*, Phys. Rev. Lett. **71,** 4022 (1993).
5. B. Meuer, D. Heitmann, K. Ploog, Phys. Rev. Lett. **68,** 1371 (1992).
6. R.B. Laughlin, Phys. Rev. B **27,** 3383 (1983).
7. W.Y. Ruan *et al.*, Phys. Rev. B **51,** 7942 (1995).
8. S.M. Girvin, T. Jach, Phys. Rev. B **29,** 5617 (1984).
9. P.A. Maksym, T. Chakraborty, Phys. Rev. Lett. **65,** 108 (1990); Phys. Rev. B **45,** 1947 (1992).
10. P. Hawrylak, Phys. Rev. Lett. **71,** 3347 (1993).
11. P. Hawrylak, D. Pfannkuche, Phys. Rev. Lett. **70,** 485 (1993).
12. T. Schmidt *et al.*, Phys. Rev. B **51,** 557 (1995).
13. S.C. Benjamin, N.F. Johnson, Phys. Rev. B **51,** 14733 (1995).
14. W.Y. Ruan, J. Math. Phys. **37,** 3760 (1996).
15. U. Merkt, J. Huser, M. Wagner, Phys. Rev. B **3,** 7320 (1991).